THERMOECONOMIC ANALYSIS OF ORGANIC RANKINE CYCLE USING ZEOTROPIC MIXTURES

Muhammad Imran[†‡], Muhammad Usman[†‡], Dong-Hyun Lee[‡] and Byung-Sik Park[*†‡]

[‡]Korea Institute of Energy Research,
152 Gajeong-ro, Yuseong-gu, Daejeon, (305-343), South Korea
Email: bspark@kier.re.kr

[†]Korea University of Science and Technology
217 Gajeong-ro Yuseong-gu, Daejeon, (305-350), South Korea
Email: imran@ust.ac.kr

* Corresponding Author: Byung-Sik Park

ABSTRACT

The selection of the working fluid is an important part of design and optimization of ORC system as it effects the systems efficiency, design of ORC components, stability, safety and environmental impact. Present study aims to investigate the performance of ORC system using pure working fluids and zeotropic mixtures for low temperature geothermal heat source on the basis of thermodynamic and economic parameters of ORC system. Evaporator, expander, condenser and feed pump models are developed in MATLAB. The control volume approach is adopted for evaporator and condenser model with appropriate database of heat transfer and pressure drop correlations. For comparison, pure working fluids are taken as the base case. The ORC system with pure working fluid and zeotropic mixture under same heat and sink source conditions are optimized using multi objective genetic algorithm for maximum exergy efficiency and minimum specific investment cost. The exergy efficiency of ORC system with zeotropic mixture is improved by 14.33% compared to pure working fluid. The exergy destruction in evaporator and condenser is reduced by 24~30%. The fraction of more volatile component in zeotropic mixture effected the thermal and economic performance of ORC system, for current study the mass fraction of 40% of R245fa corresponds to optimum exergy efficiency and specific investment cost. For same condensing pressure and expander power, area of evaporator for pure working fluids and zeotropic mixture is also calculated. The required heat transfer area for zeotropic mixture is approximately 13% less than required for pure working fluid.

1. INTRODUCTION

Organic Rankine Cycle (ORC) system effectively recovers low grade and waste heat and reduces the energy cost and environmental impact (Imran et al. 2015). Working fluid selection is considered as an important part of the design and optimization of an ORC system since the properties of the working fluid affect efficiency of system, design and size of the system components, system stability and safety, and environmental impact. During last few years, extensive research had been conducted for selection methodologies (Bao & Zhao 2013) and operating characteristics of pure working fluids for various ORC applications (Chen et al. 2010).

Liu et al. (Liu et al. 2004) found that various working fluids at specific evaporation and condensation temperatures exhibited very similar thermal efficiencies although the thermal efficiencies were found to increase slightly with the critical temperature of the working fluids. They also used two improved parameters, total heat recovery efficiency and heat availability, to evaluate the performance of an ORC system, in lieu of traditional thermal efficiency indicators. Tchanche et al. (Tchanche et al. 2009) recommended R134A as the best working fluid for low temperature solar ORC systems among the 20

working fluids investigated. Lakew and Bolland (Lakew & Bolland 2010) pointed out that the selection of working fluid depends on the nature of the heat source, temperature level and the objective function. Saleh et al. (Saleh et al. 2007) screened out the best working fluid among 31 preselected working fluids using Backone equation of state. Hung et al. (Hung et al. 1997) shed light on that different slopes and shapes of saturation vapor curves were the most crucial characteristics of working fluids for ORCs, and that isentropic fluids were the most suitable for recovering low temperature waste heat. In later research, Hung et al. (Hung et al. 2010) found dry fluids could lead to a superheated state of vapor at the exit of the expander, reducing the network area in the TS diagram, as well as increasing the cooling load of the condenser.

The second law analysis of ORC systems indicate about 70~80% of exergy destruction occurs in evaporator and condenser (Saidur et al. 2012). The non-isothermal evaporation and condensation of zeotropic working fluids makes them ideal choice for better temperature profile match between heat source, sink and working fluid and thus reducing the exergy destruction and improving the efficiency of the ORC system. Zeotropic working fluids has gained much interest in last few years (Lecompte et al. 2014). Li et al. (2014) investigated the effect of mixture composition for various working fluids and concluded that there exist an optimum value of mixture composition corresponding to highest net power output. Heberle et al. (2012) performed the second law analysis of low temperature geothermal ORC system using zeotropic mixtures. The second law efficiency was improved by 4.3%. Dong et al. (2014) investigated the effect of mixture concentration, temperature glide, pressure ratio, and condensation pressure on first and second law efficiency. Most of the recent studies (Jung et al. 2015; Li et al. 2014; Liu et al. 2014; Zhao & Bao 2014) deal with parametric performance and exergy analysis of ORC system considering the simple modeling approach for evaporator and condenser.

Since zeotropic mixtures are considered superior to pure working fluids due to their non-isothermal evaporation and condensation. Therefore, design approach of evaporator and condenser as well as appropriate heat transfer and pressure drop correlations play key role in the accurate estimation of the potential of zeotropic mixture. Present study aims to investigate the potential of zeotropic mixtures for ORC application on the basis of cycle thermodynamic performance and economic assessment considering the detailed condenser and evaporator model.

2. SYSTEM DESCRIPTION

ORC system consist of evaporator, expander, condenser and a feed pump. The schematic of ORC system and TS diagram of the pure and zeotropic working fluid are show in Fig. 1.

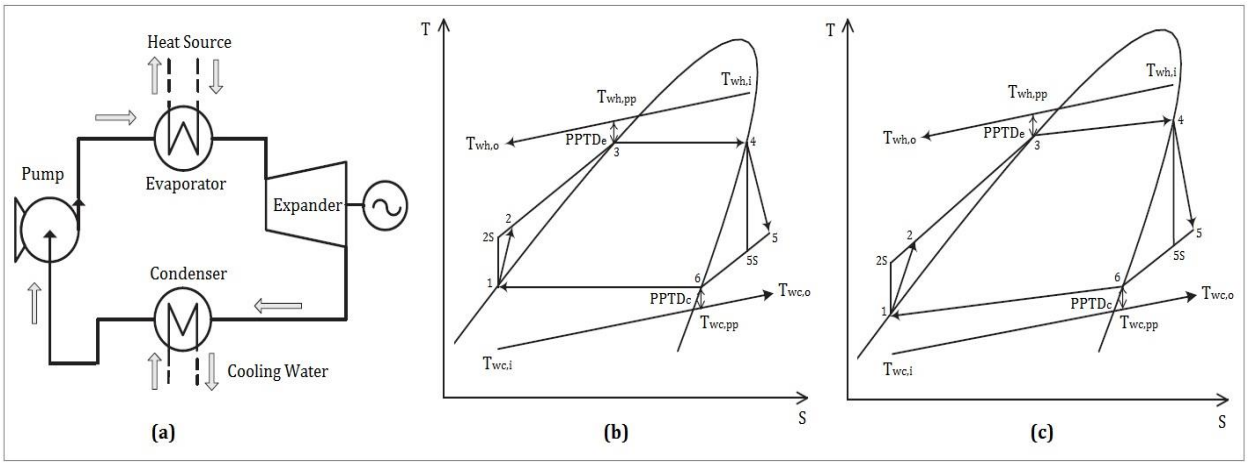

Figure 1: (a) Schematic of ORC (b) TS of pure working fluid (c) TS of zeotropic mixture

Two pure working fluids and their mixture has been considered in this study, detail of the working fluid and their characteristics are shown below in Table 1.

Table 1: Working fluid properties

Working Fluid		Physical Data				Environmental Data	
Name	Type	M (kg/kmol)	P_c (MPa)	T_c (C)	T_b (C)	ODP	GWP
Isopentane	Dry	72.15	3.380	187.2	27.8	0.00	20
R245fa	Dry	134.05	3.640	154.1	14.9	0.00	1030

For ORC design & simulation, the heat source and sink conditions are presented in Table 2.

Table 2: Design conditions of orc system for modeling and simulation

Parameter	Value	Parameter	Value
Geothermal Water, Inlet Temperature	150 C	Cooling Water, Inlet Temperature	15 C
Geothermal Water, Inlet Pressure	5 bar	Pinch point Temperature, Evaporator	10 C
Geothermal Water, Mass Flow Rate	5 kg/s	Pinch point Temperature, Condenser	7 C
Isentropic Efficiency of Turbine	75%	Isentropic Efficiency of Pump	60%

3. THERMODYNAMIC MODELING

For complete ORC system modeling, an independent model of each component, evaporator, condenser, expander and working fluid pump are developed in MATLAB. Their inputs and outputs are connected to develop the single ORC model, consisting of two parts, exergy efficiency model and specific investment cost model. The ORC model is further optimized using multi objective genetic algorithm in MATLAB optimization environment. The results of each configuration of ORC system are compared at the optimum point. The detail layout of the complete model is presented in Figure 2.

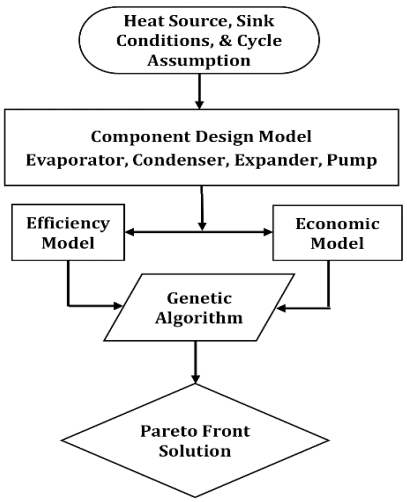

Figure 2: Detailed Layout of the optimization approach

3.1 COMPONENT MODELING

3.1.1 Evaporator Model

The evaporator is divided into three parts, subcool, two phase and superheat section. The total area of the evaporator is given by

$$A = \mathrm{n} \times A_p = n \times \left[L_p \times W_p\right] = n \times \left[\left(L_{sp} + L_{tp} + L_{sp}\right) \times W_p\right] \quad (1)$$

The total number of thermal plates are known, the plate length for each section is calculated by log mean temperature approach, the calculation process is iterative and generalized layout of the design is presented in Fig. 3.

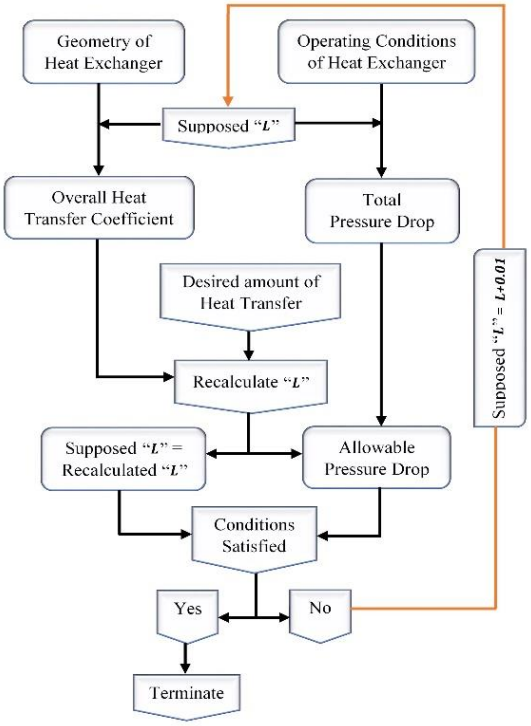

Figure 3: The design layout of plate heat exchanger

Initially, length of the plate is assumed and required plate length is recalculated based on the required amount of heat transfer, log mean temperature difference and overall heat transfer coefficient. The iterative process continues until the assumed length is equal to recalculated length.

Single Phase

The single phase Nusselt No. correlation for water in plate heat exchange is given by (Chisholm, D.; Wanniarachchi 1990)

$$Nu_w = 0.724\left(\frac{6\beta}{\pi}\right)^{0.646} Re^{0.583} Pr^{0.33} \quad (2)$$

The single phase heat transfer coefficient for pure working fluids in plate heat exchanger (Hsieh & Lin 2002)

$$\alpha_{r,sp} = 0.2092\left(\frac{k_f}{D_h}\right) Re^{0.78} Pr^{0.33}\left(\frac{\mu_m}{\mu_{wall}}\right)^{0.14} \quad (3)$$

For the zeotropic mixture, single phase heat transfer coefficient is estimated by Gnielinski correlation.

$$\alpha_{r,sp} = \frac{\left(f/8\right)(R_e - 1000)Pr}{1+12.7\left(f/8\right)^{0.5}\left(Pr^{2/3}\right)} \quad \text{where as} \quad f = [1.82\log R_e - 1.64]^{-2} \quad (4)$$

The plate length for single phase section is given by

$$L_{sp} = \frac{\mathrm{Q}_{sp}}{U_{sp} \times LMTD_{sp} \times W_p \times \mathrm{n}} \quad (5)$$

Two Phase

Since along the flow length of heat exchanger the vapor quality, temperature and concentration changes, therefore, control volume approach was adopted for evaporator modeling. The two phase section of evaporator is discretized and divided into N parts. The thermodynamic properties in each part are assumed constant and the variation in temperature difference is linear. The discretized temperature profile of two phase section of evaporator is shown in Fig. 4.

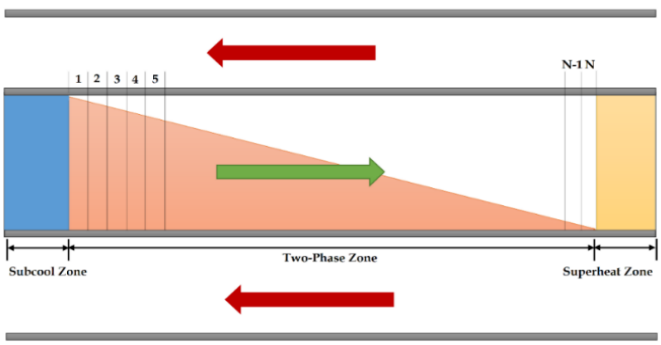

Figure 4: Control volume of two phase section of evaporator

The convective heat transfer coefficient for R245fa in plate heat exchanger (D. H. Han et al. 2003)

$$N_U = G_{e1} {Re_{eq}}^{G_{e2}} {Bo_{eq}}^{0.3} Pr^{0.4} \quad (6)$$

where as

$$G_{e1} = 2.81\left(\frac{P_{co}}{D_h}\right)^{-0.041}\left(\frac{\pi}{2}-\beta\right)^{-2.83};\ G_{e2} = 2.81\left(\frac{P_{co}}{D_h}\right)^{-0.082}\left(\frac{\pi}{2}-\beta\right)^{0.61} \quad (7)$$

The equivalent Reynolds number and boiling number is given by

$$Re_{eq} = \frac{G_{eq} D_h}{\mu_f};\ Bo_{eq,i} = \frac{q^{"}}{G_{eq} \times i_{fg}};\ G_{eq} = G\left[1 - x + x\left(\frac{\rho_f}{\rho_g}\right)^{0.5}\right] \quad (8)$$

While two phase frictional factor is given by (D. H. Han et al. 2003)

$$f = G_{e3} {Re_{eq}}^{G_{e4}} \quad (9)$$

where as

$$G_{e3} = 64710\left(\frac{P_{co}}{D_h}\right)^{-5.27}\left(\frac{\pi}{2}-\beta\right)^{-3.03};\ G_{e4} = -1.314\left(\frac{P_{co}}{D_h}\right)^{-0.62}\left(\frac{\pi}{2}-\beta\right)^{-0.47} \quad (10)$$

For the zeotropic mixture, two phase heat transfer coefficient is estimated by Jung's Correlation (Jung et al. 1989).

$$\alpha_{tp} = \frac{S}{C_{UN}} h_{UN} + C_{me} F h_l,\ S = \begin{cases} 4048 X_{tt}^{1.22} Bo^{1.13}, if & X_{tt} < 1 \\ 1 - 0.1 X_{tt}^{-0.28} Bo^{-0.33}, if & 1 < X_{tt} < 5 \end{cases},\ C_{UN} = |1 + (b_2 + b_3)(1 + b_4)|(1 + b_5)$$

$$b_2 = (1 - X)\ln\left(\frac{1.01 - X}{1.01 - Y}\right) + X\ln\left(\frac{X}{Y}\right) + |Y - X|^{1.5},\ b_3 = \begin{cases} 0, if & X \geqslant 0.01 \\ (Y/X)^{0.1} - 1, if & X < 0.01 \end{cases},$$

$$b_4 = 152(p/p_c)^{3.9}, b_5 = 0.92|Y - X|^{0.001}(p/p_c)^{0.66}, X/Y = 1, if\ X = Y = 0 \quad (11)$$

$$h_{UN} = \frac{1}{C_{UN}} \frac{h_1 h_2}{h_1 X_1 + h_2 X_2}, h_i = 207 \frac{k_l}{d}\left(\frac{q d_e}{k_l T_{sat}}\right)^{0.745}\left(\frac{\rho_G}{\rho_L}\right) \mathrm{Pr}_l^{0.533}, d_e = 0.0146 \times 35[2\sigma/(g(\rho_L - \rho_G))]^{0.5}$$

$$C_{me} = 1 - 0.35|Y - X|^{1.56}, F = 2.37[0.29 + \frac{1}{X_{tt}}]^{0.85}, h_l = 0.023 \frac{k_l}{d} \mathrm{Re}_L^{0.8} \mathrm{Pr}^{0.4}$$

The plate length for two phase section is given by

$$L_{tp} = \frac{\sum_{i=1}^{N} \mathrm{Q}_{(tp,i)}}{U_{(tp,i)} \times LMTD_{(tp,i)} \times W_p \times \mathrm{n}} \quad (12)$$

3.1.2 Condenser Model

The condenser model is similar to the evaporator model except the heat transfer correlation during condensation. For water side the heat same transfer correlations were used while for two phase condensation of pure working fluids is given by (D. Han et al. 2003).

$$Nu = Ge_5 {Re_{eq}}^{Ge_6} {Bo_{eq}}^{0.3} Pr^{0.4} \quad (13)$$

Where as

$$Ge_5 = 11.22\left(\frac{P_{co}}{D_h}\right)^{-0.041}\left(\frac{\pi}{2}-\beta\right)^{-4.5};\ Ge_6 = 0.35\left(\frac{P_{co}}{D_h}\right)^{0.23}\left(\frac{\pi}{2}-\beta\right)^{1.48} \quad (14)$$

For the zeotropic mixture, two phase condensation heat transfer coefficient is estimated by (Del Col et al. 2005).

$$\alpha_{tp} = \frac{\alpha_{f,m}\theta + (2\pi-\theta)\alpha_{c,m}}{2\pi},\ \theta = \begin{cases} \theta_{strat}, if\ G < G_{strat} \\ \theta_{strat}\left(\frac{G_{wavy}-G}{G_{wavy}-G_{strat}}\right)^{0.5}, if\ G_{strat} < G < G_{wavy} \\ 0, else \end{cases},\ \alpha_{c,m} = \left(R_c + \frac{1}{\alpha_c}\right)^{-1}$$

$$\alpha_c = 0.003\mathrm{Re}_L^{0.74}\mathrm{Pr}_L^{0.5}\frac{\lambda_L}{\delta}f_i,\ f_i = \begin{cases} 1 + \left(\frac{u_G}{u_L}\right)^{0.5}\left[\frac{(\rho_L-\rho_G)g\delta^2}{\sigma}\right]^{0.25}, & G > G_{strat} \\ 1 + \left(\frac{u_G}{u_L}\right)^{0.5}\left[\frac{(\rho_L-\rho_G)g\delta^2}{\sigma}\right]^{0.25}\frac{G}{G_{strat}}, & G < G_{strat} \end{cases} \quad 15$$

$$R_c = xC_{pG}\frac{\Delta T_{gl}}{\Delta h_m}\frac{1}{\alpha_G^O},\ \alpha_G^O = \alpha_G f_i,\ \alpha_G = \frac{\lambda_G}{d}0.023\mathrm{Re}_G^{0.8}\mathrm{Pr}_G^{0.33}$$

$$\alpha_{f,m} = F_m(R_f + \frac{1}{\alpha_f})^{-1},\ \alpha_f = 0.728\left[\frac{\rho_L(\rho_L-\rho_G)gh_{LV}\lambda_L^3}{\mu_L d(T_{sat}-T_w)}\right]^{0.25},\ R_f = xC_{pG}\frac{\Delta T_{gl}}{\Delta h_m}\frac{1}{\alpha_G}$$

$$F_m = \exp\left[-0.25(1-x)\left(\frac{G_{wavy}}{G}\right)^{0.5}\frac{\Delta T_{gl}}{T_{sat}-T_w}\right]$$

3.2 Energy & Exergy Analysis

Network and thermal efficiency of the ORC system is given by

$$\mathrm{W}_{net} = \dot{m}[(h_4 - h_5) - (h_2 - h_1)] \quad ; \quad \eta_{\mathrm{thermal}} = \frac{\mathrm{W}_{net}}{\mathrm{Q}_{evp}} \times 100 \quad 16$$

The physical exergy at i_{th} point of j_{th} component of ORC system is given by

$$\epsilon_{i,j} = \epsilon_{Phy} = \dot{m}[(h - h_o) - T_o(s - s_o)] \quad 17$$

The exergy loss and exergy efficiency of the ORC component is shown in Table 3

Table 3: Exergy loss and exergy efficiency of orc components

Component	Available Exergy	Used Exergy	Exergy Loss	Exergy Efficiency
Pump	W_p	$\epsilon_2 - \epsilon_1$	$\epsilon_t = \mathrm{W}_p - (\epsilon_2 - \epsilon_1)$	$\frac{\epsilon_2 - \epsilon_1}{\mathrm{W}_p}$
Evaporator	$\epsilon_{wh,i} - \epsilon_{wh,o}$	$\epsilon_4 - \epsilon_2$	$\epsilon_e = (\epsilon_{wh,i} - \epsilon_{wh,o}) - (\epsilon_4 - \epsilon_2)$	$\frac{(\epsilon_4 - \epsilon_2)}{(\epsilon_{wh,i} - \epsilon_{wh,o})}$
Turbine	W_t	$\epsilon_4 - \epsilon_5$	$\epsilon_p = \mathrm{W}_t - (\epsilon_4 - \epsilon_5)$	$\frac{\epsilon_4 - \epsilon_5}{\mathrm{W}_t}$
Condenser	$\epsilon_5 - \epsilon_1$	$\epsilon_{wc,i} - \epsilon_{wc,o}$	$\epsilon_c = (\epsilon_5 - \epsilon_1) - (\epsilon_{wc,i} - \epsilon_{wc,o})$	$\frac{(\epsilon_{wc,i} - \epsilon_{wc,o})}{(\epsilon_5 - \epsilon_1)}$

The exergy efficiency of the system is given by

$$\eta_{exergy} = \frac{\sum \epsilon_{used}}{\sum \epsilon_{available}} = \frac{W_n}{\epsilon_e + \epsilon_p} \quad 18$$

4. ECONOMIC MODELING

Bare module cost method is one of the reasonable cost estimation approach for power plant equipment (Turton 2009) and has been used for cost estimation of ORC system as well (Imran et al. 2014; Wang et al. 2013). Generalized cost correlation of individual components ORC is given by

$$\mathrm{Cost}\ (\$) = \frac{\mathrm{CEPCI}_{2014}}{\mathrm{CEPCI}_{1996}} \times F_S \times \acute{C}_b \times \{B_1 + (B_2 \times F_M \times F_P)\} \quad 19$$

Basic cost, $\acute{C}_b$, of the components is given by

$$\log \acute{C}_b = \{K_1 + K_2(\log Z) + K_3(\log Z)^2\} \quad 20$$

The pressure factor for heat exchanger is given by

$$\log F_P = \{C_1 + C_2(\log P) + C_3(\log \mathrm{P})^2\} \quad 21$$

Total cost, C_T is the sum of cost of evaporator, condenser, expander and working fluid pump. The specific investment cost (SIC) of ORC system is given by

$$\mathrm{SIC}(\$/_{kW}) = \frac{[C_T + OMC]}{[W_{net}]} \quad 22$$

Whereas OMC is operation and maintenance cost and is taken as 30% of total cost (Quoilin et al. 2011).

5. OPTIMIZATION APPROACH

The individual model of ORC components are connected in MATLAB with thermal and economic model. For pure and zeotropic working fluids, the ORC system was optimized for minimum specific investment and maximum exergy efficiency under logical bound of evaporation temperature, mass fraction of more volatile component and pinch point temperature in evaporator. The optimization was performed using multi objective genetic algorithm. The results of optimization of ORC system with pure and zeotropic working fluid are compared.

6. RESULTS AND DISCUSSION

There is trade off between exergy efficiency and specific investment cost so single value of decision variables cannot satisfy both objective functions simultaneously. Therefore, optimization results are presented in the Pareto Front form as shown in Table 4 and Fig. 5.

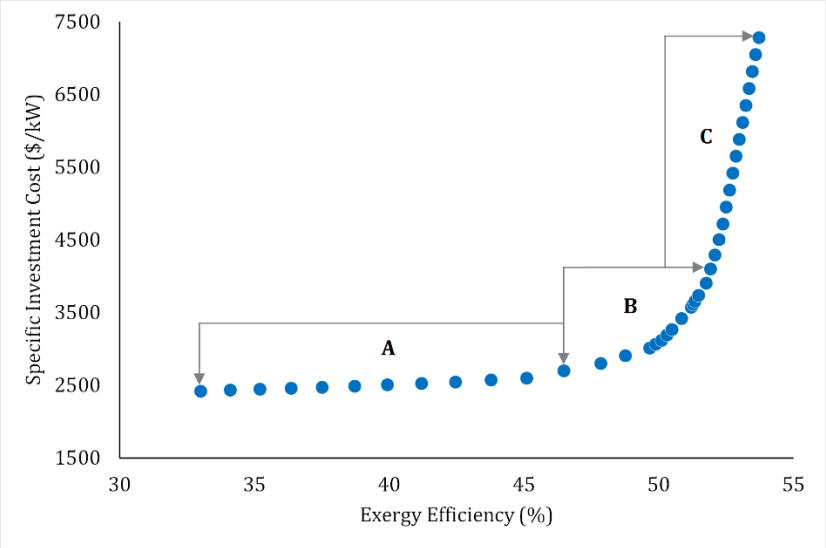

Figure 5: Pareto Front Solution of ORC system for zeotropic mixture

After the optimum operating point B, there is sharp increase in specific investment cost with slight increase in exergy efficiency. The optimization results in Table 3 shows that the exergy efficiency of ORC system with zeotropic mixture is 13.7% higher than ORC system with R245fa and 26.6% higher than R601a. From point A to point B the exergy efficiency has improved significantly with slight increase in specific investment cost, from point B to point C there is slight increase in exergy efficiency while there is sharp increase in specific investment cost. Pint A present the low SIC and low efficiency, point C represent high SIC and high exergy efficiency, whereas point B shows the optimum range of exergy efficiency and SIC.

Table 4: Pareto Front Solution of ORC system with pure and zeotropic working fluids

Working Fluid	Optimized Parameters			Objective Functions		Cycle Performance	
	Mass Fraction	Evaporation Pressure	Pinch Pint Evaporator	Specific Investment Cost	Exergy Efficiency	Thermal Efficiency	Temperature Glide
	%	bar	C	$/kW	%	%	C
R245fa	100	10.45	8.50	3692	44.73	8.79	0.00
R601a	100	6.15	9.20	3857	40.15	9.89	0.00
R245fa+R601a	40+60	8.45	8.25	3416	50.85	10.06	6.16

Based on the Pareto Front solution, under considered conditions an empirical correlation has been developed for specific investment cost.

$$SIC\left(\$/_{kW}\right) = 0.078\eta^4 - 9.78\eta^3 + 403.13\eta^2 - 5403.38\eta \quad (23)$$

Empirical correlation is valid within given range of operating condition, and exergy efficiency

$$33\% \leq \eta_{ex} \leq 54\% \quad (24)$$

The exergy destruction for each working fluid is calculated at their optimum evaporation temperature and mass fraction. The exergy destruction and irreversibilities in ORC are shown in Fig. 6. The maximum exergy destruction occurs in evaporator and condenser, accounts more than 70% of total system exergy loss.

ORC system with zeotropic mixture has 21% less exergy destruction in evaporator and 28% less exergy destruction in condenser compare to ORC system with pure working fluid R601a and R245fa respectively.

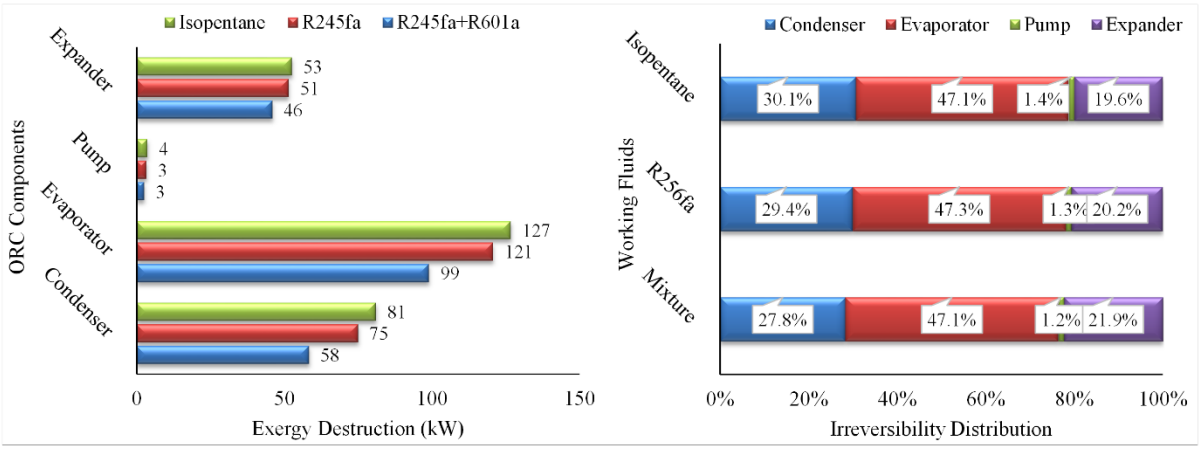

Figure 6: Exergy destruction of ORC components and irreversibilities distribution of ORC system

The effect of the evaporation temperature and mass fraction of more volatile component on exergy efficiency and specific investment has been estimated, as shown in Fig. 7.

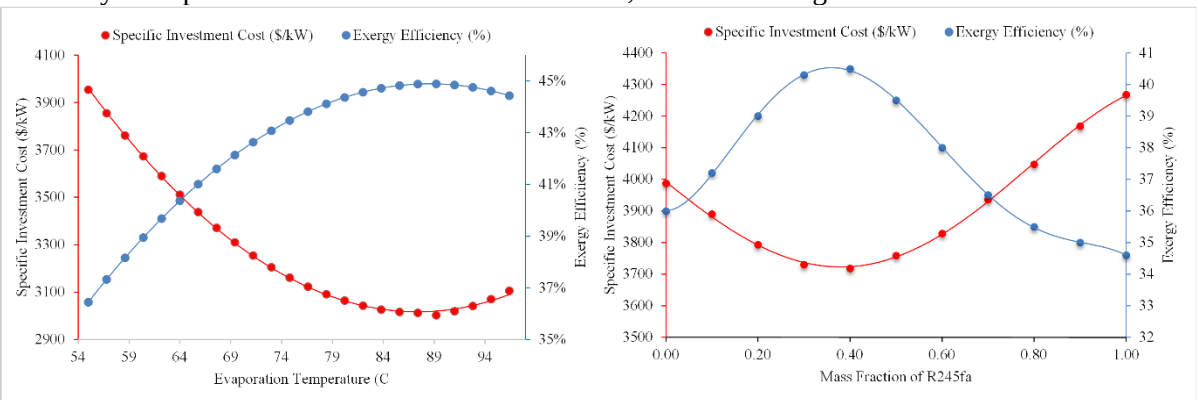

Figure 7: Effect of evaporation temperature and mass fraction of R245fa on exergy efficiency and SIC

With increase in evaporation temperature, the net power increase initially and after optimum evaporation temperature it start to decrease. As a result the SIC decrease with increase in evaporation temperature and after optimum evaporation temperature again start increasing. Since exergy efficiency is affected by both the net power output and total exergy destruction. Therefore exergy efficiency increases due to increase in net power and decrease in exergy destruction. However at elevated evaporation temperature the increase in exergy efficiency is not so sharp due to decrease in net power.
There is an optimum value of mass fraction of more volatile component where the temperature glide is maximum and so the exergy efficiency and net power. At 40% mass fraction of R245fa the temperature glide was maximum, 6.16C, therefore, the exergy loss in evaporator and condenser was minimum. Similar trend was observed for net power of ORC system, the maximum power is observed at 40% mass fraction of R245fa. The net power decreased before and after the optimum value, 40%, of R245fa mass fraction. Therefore, the specific investment cost ORC system is minimum at optimum mass fraction of more volatile component R245fa.
Since the major advantage of zeotropic mixture is achieved in evaporator and condenser, therefor, for economic point of view, the evaporator and condenser area is estimated for each pure working fluid and zeotropic mixture. Under constant condensing temperature, degree of subcooling and turbine power, total heat transfer area of evaporator and condenser is estimated. Results of the comparison is shown in Table 5.

Table 5: Heat transfer area of evaporator & condenser

Component	**Heat Transfer Area (m^2)**		
	R245fa	**R601a**	**R245fa-R601a**
Evaporator	128	138	121
Condenser	141	144	126

7. CONCLUSIONS

Simulation study has been performed for the potential of zeotropic mixture application in ORC system and the results are compared with ORC using pure working fluids. Following conclusions can be drawn from the study. Due to non-isothermal evaporation and condensation, the exergy loss in evaporator and condenser is reduced considerably. The ORC system with zeotropic mixture has better exergy efficiency, 14.33% higher than ORC using pure working fluids. The overall exergy destruction has been reduced by 21% using the zeotropic mixture as working fluid. The composition of the mixture has an important effect on the ORC system performance, which is always associated with the temperature glide during the phase change of the mixture. Consequently, an optimal mixture concentration exists which maximizes the second law efficiency. For current study the optimum mass fraction of R245a is 40%. For constant condensing temperature, heat source amount and turbine power, required heat transfer area of evaporator and condenser using zeotropic mixture is relatively small compare to pure working fluids. The heat transfer area of evaporator and condenser has been reduced by 13% and 12% respectively. Although a number of studies have been conducted on zeotropic mixture but only limited experimental data is available about two phase heat transfer of zeotropic working fluids. Moreover the effect of composition shift has not been widely explored which is caused by the differential hold up in evaporator and condenser. Further experimentation of two phase heat transfer and data base of mixture properties is essential for accurate modeling of ORC system with zeotropic mixtures.

NOMENCLATURE

A	area, m^2	U	overall heat transfer coefficient, $W.m^{-2}.K^{-1}$
B_o	boiling number	n	no. of thermal plates
CEPCI	chemical engineering plant cost index	Nu	Nusselt number
C_p	Specific Heat Capacity, J/kg.K	P	pressure, Pa
D_h	hydraulic diameter, m	Pr	Prandtl number
f	friction factor	q'	average heat flux, $W.m^{-2}$

G	mass velocity, $kg.m^{-1}.s^{-1}$		
G_{start}	stratified flow transition mass velocity	Q	heat transfer rate, kW
G_{wavy}	wavy flow transition mass velocity	Re	Reynolds number
h	Specific Enthalpy, kJ/kg	SIC	Specific investment cost, $/kW
i_{fg}	enthalpy of vaporization, $J.kg^{-1}$	T	temperature, ℃
k	thermal conductivity, $W.m^{-1}.K^{-1}$	x	liquid phase mass fraction
$LMTD$	Log mean temperature difference, ℃	X_{tt}	Martinelli parameter
$\dot{m}$	mass flow rate, $kg.s^{-1}$	y	vapor phase mass fraction

Subscripts

eq	equivalent
f	liquid phase
g	vapor phase
p	plate
w	water
r	refrigerant side
sp	single phase
tp	two phase
f	liquid phase
g	vapor phase
w	water side

Greek Letters

β	chevron angel, degree
$\in$	Physical exergy, kJ
ρ	density, $kg.m^{-3}$
μ	viscosity, $kg.s^{-1}.m^{-1}$
η	Efficiency
α	Heat transfer coefficient, $W/m^2.K$
θ	Falling film angle

REFERENCES

Bao, J. & Zhao, L., 2013. A review of working fluid and expander selections for organic Rankine cycle. Renewable and Sustainable Energy Reviews, 24, pp.325–342.

Chen, H., Goswami, D.Y. & Stefanakos, E.K., 2010. A review of thermodynamic cycles and working fluids for the conversion of low-grade heat. Renewable and Sustainable Energy Reviews, 14(9), pp.3059–3067.

Chisholm, D.; Wanniarachchi, A.S., 1990. 9. In AIChE SPRING NATIONAL MEETING. ORLANDO, FL.

Del Col, D., Cavallini, a. & Thome, J.R., 2005. Condensation of Zeotropic Mixtures in Horizontal Tubes: New Simplified Heat Transfer Model Based on Flow Regimes. Journal of Heat Transfer, 127(3), p.221.

Dong, B. et al., 2014. Analysis of zeotropic mixtures used in high-temperature Organic Rankine cycle. Energy Conversion and Management, 84, pp.253–260.

Han, D., Lee, K. & Kim, Y., 2003. The characteristics of condensation in brazed plate heat exchangers with different chevron angles. JOURNAL-KOREAN PHYSICAL SOCIETY, 43(1), pp.66–73.

Han, D.H., Lee, K.J. & Kim, Y.H., 2003. Experiments on the characteristics of evaporation of R410A in brazed plate heat exchangers with different geometric configurations. Applied Thermal Engineering, 23(10), pp.1209–1225.

Heberle, F., Preißinger, M. & Brüggemann, D., 2012. Zeotropic mixtures as working fluids in Organic Rankine Cycles for low-enthalpy geothermal resources. Renewable Energy, 37(1), pp.364–370.

Hsieh, Y.Y. & Lin, T.F., 2002. Saturated flow boiling heat transfer and pressure drop of refrigerant R-410A in a vertical plate heat exchanger. International Journal of Heat and Mass Transfer, 45(5), pp.1033–1044.

Hung, T.C. et al., 2010. A study of organic working fluids on system efficiency of an ORC using low-grade energy sources. Energy, 35(3), pp.1403–1411.

Hung, T.C., Shai, T.Y. & Wang, S.K., 1997. A review of organic rankine cycles (ORCs) for the recovery of low-grade waste heat. Energy, 22(7), pp.661–667.

Imran, M. et al., 2015. Economic assessment of greenhouse gas reduction through low-grade waste heat recovery using organic Rankine cycle (ORC). Journal of Mechanical Science and Technology, 29(2), pp.835–843.

Imran, M. et al., 2014. Thermo-economic optimization of Regenerative Organic Rankine Cycle for waste heat recovery applications. Energy Conversion and Management, 87, pp.107–118.

Jung, D.S. et al., 1989. Horizontal flow boiling heat transfer experiments with a mixture of R22 / R114. International Journal of Heat and Mass Transfer, 32(1), pp.131–145.

Jung, H.C., Taylor, L. & Krumdieck, S., 2015. An experimental and modelling study of a 1 kW organic Rankine cycle unit with mixture working fluid. Energy.

Lakew, A.A. & Bolland, O., 2010. Working fluids for low-temperature heat source. Applied Thermal Engineering, 30(10), pp.1262–1268.

Lecompte, S. et al., 2014. Exergy analysis of zeotropic mixtures as working fluids in Organic Rankine Cycles. Energy Conversion and Management, 85, pp.727–739.

Li, Y.-R. et al., 2014. Potential of organic Rankine cycle using zeotropic mixtures as working fluids for waste heat recovery. Energy, 77, pp.509–519.

Liu, B.T., Chien, K.H. & Wang, C.C., 2004. Effect of working fluids on organic Rankine cycle for waste heat recovery. Energy, 29(8), pp.1207–1217.

Liu, Q., Duan, Y. & Yang, Z., 2014. Effect of condensation temperature glide on the performance of organic Rankine cycles with zeotropic mixture working fluids. Applied Energy, 115, pp.394–404.

Quoilin, S. et al., 2011. Thermo-economic optimization of waste heat recovery Organic Rankine Cycles. Applied Thermal Engineering, 31(14-15), pp.2885–2893.

Saidur, R. et al., 2012. Exergy analysis of solar energy applications. Renewable and Sustainable Energy Reviews, 16(1), pp.350–356.

Saleh, B. et al., 2007. Working fluids for low-temperature organic Rankine cycles. Energy, 32(7), pp.1210–1221.

Tchanche, B.F. et al., 2009. Fluid selection for a low-temperature solar organic Rankine cycle. Applied Thermal Engineering, 29(11-12), pp.2468–2476.

Turton, R., 2009. Analysis, Synthesis, and Design of Chemical Processes, Prentice Hall. Available at: http://books.google.com/books?id=YEJHAQAAIAAJ.

Wang, J. et al., 2013. Multi-objective optimization of an organic Rankine cycle (ORC) for low grade waste heat recovery using evolutionary algorithm. Energy Conversion and Management, 71, pp.146–158.

Zhao, L. & Bao, J., 2014. Thermodynamic analysis of organic Rankine cycle using zeotropic mixtures. Applied Energy, 130, pp.748–756.

ACKNOWLEDGEMENTS

The authors gratefully acknowledge the financial support provided by the Korea Institute of Energy Research and Korea University of Science and Technology (B4-5524).